HHS Public Access

Author manuscript

*Mol Pharm*. Author manuscript; available in PMC 2016 October 05.

Published in final edited form as:

*Mol Pharm*. 2015 October 5; 12(10): 3518–3526. doi:10.1021/acs.molpharmaceut.5b00054.

# Reductively Responsive Hydrogel Nanoparticles with Uniform Size, Shape, and Tunable Composition for Systemic siRNA Delivery *in Vivo*

**Da Ma**[#†,‡], **Shaomin Tian**[#‡,§,¶], **Jeremy Baryza**[‖], **J. Christopher Luft**[‡,§,▲], and **Joseph M. DeSimone**[*,†,‡,§,○,▲,◆,●,■,□]

[†]Department of Chemistry, University of North Carolina, Chapel Hill, North Carolina 27599, United States

[‡]Lineberger Comprehensive Cancer Center, University of North Carolina, Chapel Hill, North Carolina 27599, United States

[¶]Department of Microbiology & Immunology, University of North Carolina, Chapel Hill, North Carolina 27599, United States

[§]Carolina Center of Cancer Nanotechnology Excellence, University of North Carolina, Chapel Hill, North Carolina 27599, United States

[‖]Novartis Institutes for BioMedical Research, Cambridge, Massachusetts 02139, United States

[○]Department of Pharmacology, University of North Carolina, Chapel Hill, North Carolina 27599, United States

[▲]Eshelman School of Pharmacy, University of North Carolina, Chapel Hill, North Carolina 27599, United States

[◆]Institute for Advanced Materials, University of North Carolina, Chapel Hill, North Carolina 27599, United States

[●]Institute for Nanomedicine, University of North Carolina, Chapel Hill, North Carolina 27599, United States

[■]Department of Chemical and Biomolecular Engineering, North Carolina State University, Raleigh, North Carolina 27695, United States

[□]Sloan-Kettering Institute for Cancer Research, Memorial Sloan-Kettering Cancer Center, New York, New York 10021, United States

[*]**Corresponding Author**desimone@unc.edu..

Present Address

D.M.: 220 Handan Road, Department of Chemistry, Fudan University, Shanghai, China 200433.

Supporting Information

The Supporting Information is available free of charge on the ACS Publications website at DOI: 10.1021/acs.molpharmaceut.5b00054. Representative “blank” nanoparticle composition and SEM image, “post-fabrication” siRNA loading method, methods for siRNA modification and mPEG-PAA preparation, additional cell assay, and experimental details for *in vivo* assays (PDF)

Notes

The authors declare the following competing financial interest(s): Joseph DeSimone is a founder and maintains a financial interest in Liquidia Technologies. Liquidia was founded in 2004 to commercialize PRINT technology and other discoveries of Professor Joseph DeSimone and colleagues at the University of North Carolina, Chapel Hill.

[#] These authors contributed equally to this work.


## Abstract

To achieve the great potential of siRNA based gene therapy, safe and efficient systemic delivery *in vivo* is essential. Here we report reductively responsive hydrogel nanoparticles with highly uniform size and shape for systemic siRNA delivery *in vivo*. "Blank" hydrogel nanoparticles with high aspect ratio were prepared using continuous particle fabrication based on PRINT (particle replication in nonwetting templates). Subsequently, siRNA was conjugated to "blank" nanoparticles via a disulfide linker with a high loading ratio of up to 18 wt %, followed by surface modification to enhance transfection. This fabrication process could be easily scaled up to prepare large quantity of hydrogel nanoparticles. By controlling hydrogel composition, surface modification, and siRNA loading ratio, siRNA conjugated nanoparticles were highly tunable to achieve high transfection efficiency *in vitro*. FVII-siRNA conjugated nanoparticles were further stabilized with surface coating for *in vivo* siRNA delivery to liver hepatocytes, and successful gene silencing was demonstrated at both mRNA and protein levels.


## Abstract

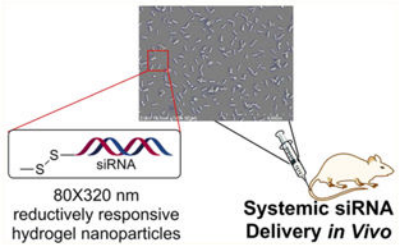



### Keywords

drug delivery; gene therapy; nanoparticles; hydrogel; siRNA


## 1. INTRODUCTION

RNA interference (RNAi) with small interfering RNA (siRNA) is a promising biotechnology, which has great potential to treat cancer and other diseases.[1–3] As a negatively charged biological molecule, naked siRNA is unable to penetrate the cell membrane effectively.[4] In addition, siRNA is unstable and susceptible to degradation by RNase in serum. A safe and efficient delivery method is necessary to protect siRNA and facilitate its delivery to the cytoplasm. A suitable delivery carrier should assist in overcoming multiple biological barriers for systemic delivery *in vivo*, to enable prolonged circulation time, target-specific cellular uptake, and enhanced endosomal escape.[5] Nanoparticles are of extreme interest for siRNA delivery as a result of the ease to control particle composition and surface properties. Different types of nanoparticles have been developed to deliver siRNA, which include lipid nanoparticles,[6–17] polymer-based nanoparticles,[18–23] peptide-based nanoparticles,[24,25] calcium phosphate nanoparticles,[26,27] and other inorganic nanoparticles.[28,29] Nevertheless, it remains a challenge to achieve systemic delivery *in vivo*. To date, there are only a few examples of systemic siRNA delivery

*in vivo* with lipids,[6–8] cationic polymers,[3,30] and lipid-coated calcium phosphate.[26,31] The majority of these examples are based on physical entrapment of siRNA, which may lead to premature release during blood circulation.

Particle replication in nonwetting templates (PRINT) is a particle fabrication technology capable of producing nano-particles or microparticles with highly uniform shape, size, and composition.[32–36] We previously reported the use of PRINT based hydrogel nanoparticles to deliver siRNA *in vitro*.[37] In that work, siRNA was loaded when nanoparticles were being fabricated, requiring water to be used as solvent (see further explanations in Supporting Information, Part 2), which does not favor continuous particle fabrication process. Therefore, batch fabrication method was used. To enable the full potential of PRINT technology by using continuous particle fabrication[38] to efficiently produce large quantity of highly uniform particles, we developed a new "post-fabrication" siRNA loading method. With this new method, reductively responsive nanoparticles were efficiently prepared with continuous fabrication process. The loading efficiency of siRNA was also greatly improved. The resulting luciferase-siRNA conjugated nanoparticles were able to efficiently knock down luciferase expression *in vitro*. Furthermore, the surface of nanoparticles were modified to facilitate systemic delivery of siRNA *in vivo*, and efficient gene silencing of FVII in liver hepatocytes was achieved with FVII-siRNA conjugated nanoparticles.

## 2. MATERIALS

Tetraethylene glycol monoacrylate ($HP_4A$) was synthesized in house[39] and kindly provided by Dr. Ashish Pandya and Mathew Finnis. DMAPMA (*N*-[3-(dimethylamino)propyl]-methacrylamide) was from TCI America. 2-(Methacryloyloxy)-ethyltrimethylammonium chloride solution, poly(acrylic acid) ($M_w$ = 1800), *S*-acetylthioglycolic acid *N*-hydroxysuccinimide ester, and TPO (diphenyl(2,4,6-trimethylbenzoyl)phosphine oxide) were from Sigma-Aldrich. $mPEG_{5k}$ acrylate and $mPEG_{5k}$-$NH_2$ were from CreativePEGWorks. NHS-$PEG_{3.4k}$-COOH was from Laysan Bio. Poly-L-lysine hydrobromide and DL-dithiothreitol were from Sigma. EDC (1-ethyl-3-(3-(dimethylamino)propyl)carbodiimide hydrochloride), hydrox-ylamine hydrochloride and SPDP were from Thermo Scientific. AEM (2-aminoethyl methacrylate hydrochloride) and $PEG_{700}$ diacrylate were from Acros Organics. Sulfo-NHS (*N*-hydrox-ysulfosuccinimide sodium salt) was from Chem-Impex International. Sense strand amine modified siRNA was synthesized by Novartis. The sequences of siRNA: Luciferase sense amine-modified 5′-$NH_2$-C6-GAUUAUGUCCGGUUAUGUAUU-3′. antisense 5′-UACAUAACCGGACAUAAUCUU-3′; FVII sense 5′-$NH_2$-C6-uGucuuGGuuucAAuuAAAuu; antisense 5′-UUuAAUUGAAACcAAGAcAuu-3′. Luciferase siRNA was used as control for *in vivo* experiments in mice, and FVII siRNA was used as control for *in vitro* assays on HeLa/luc cells.

## 3. EXPERIMENTAL METHODS

### 3.1. "Blank" Nanoparticle Fabrication

The method for nanoparticle fabrication on a PRINT based continuous particle fabrication instrument was described in detail previously.[40] The preparticle solution was prepared by

dissolving 5 wt % of the various reactive monomers in methanol. A representative preparticle solution composition was shown in Table S1. Nanoparticles were transferred to plasdone harvest sheets and harvested with sterile water with a yield of 0.8 mg/foot. SEM micrograph of "blank" nanoparticles was shown in Figure S1. DyLight 680 labeled nanoparticles were prepared similarly with the addition of DyLight 680 succimide.

### 3.2. siRNA Loading and Nanoparticle Surface Modification

First, "Blank" nanoparticles were suspended in anhydrous DMF at 2 mg/mL. NHS-$PEG_{3.4k}$-COOH (1 equiv to nanoparticle mass) and pyridine (2 equiv to nanoparticle mass) were added. The reaction proceeded at r.t. for 12 h, followed by centrifugation (14 000 rpm, 20 min, 4 °C) to collect nanoparticles. Next, nanoparticles were resuspended in PBS at 2 mg/mL and SPDP (0.2 equiv to nanoparticle mass in $CH_3CN$) was added. The suspension was vortexed gently at r.t. for 6 h. Nanoparticles were collected by centrifugation (14 000 rpm, 20 min, 4 °C) and subsequently washed twice with sterile water. Subsequently, siRNA-SH (synthetic procedure was described in Supporting Information) was added to a suspension of nanoparticles (10 mg/mL) in PBS, which was shaken at r.t. for 12 h. Nanoparticles conjugated with siRNA were collected by centrifugation (14 000 rpm, 20 min, 4 °C), which were washed twice with 10× PBS and twice with sterile water. Finally, nanoparticles were suspended in PBS (1 mg/mL). EDC (3 equiv), sulfo-NHS (10 equiv), and PLL (10 equiv) were added. Reaction proceeded at r.t. for 12 h. Nanoparticles were centrifuged and washed once with 10× PBS and twice with sterile water. The resulting hydrogel nanoparticles were used for cellular study *in vitro*. To conduct hemolysis assay and deliver siRNA *in vivo*, nanoparticles (4 mg/mL) were incubated in a solution of m$PEG_{5k}$-PAA (synthetic procedure was described in Supporting Information, 10 equiv in PBS) for 30 min. Resulting nanoparticles were collected with centrifugation (14 000 rpm, 20 min, 4 °C) and washed once with PBS.

### 3.3. Nanoparticle Characterization

Scanning electron microscopy (SEM) enabled imaging of hydrogels that were dispersed on a silicon wafer and coated with 2.2 nm of Au/Pd (Hitachi S-4700). $\xi$-potential and dynamic light scattering measurements (approximate measurements of hydrogel dynamic size of rod-like particles based on a mathematical model of spherical particles) were conducted on 20 $\mu$g/mL particle dispersions in 1 mM KCl or 0.1× PBS buffer using a Zetasizer Nano ZS particle analyzer (Malvern Instruments Inc.).

### 3.4. Analysis of siRNA by Gel Electrophoresis

2.5% agarose gel in TBE buffer was prepared with 0.5 $\mu$g/mL of ethidium bromide. To study release of siRNA from hydrogel nanoparticles, nanoparticles were incubated in 1× PBS, with 5 mM reduced glutathione (GSH). Aliquots of particle dispersions were centrifuged (14 000 rpm, 15 min, 4 °C) for recovery of the supernatant at various time points which were then stored at −20 °C until analysis on gel. For evaluation of protection of siRNA by nanoparticles, siRNA hydrogels were incubated in 1× PBS supplemented with 30% FBS at 37 °C for given times, followed by incubation in 10× PBS (5 mM glutathione) for 4 h at 1.2 mg/mL and 37 °C to release all siRNA. Twelve microliters of sample (supernatants from particle dispersions, siRNA solutions, or particle dispersions) was mixed with 3 $\mu$L of 6×

loading buffer (60% glycerol, 0.12 M EDTA in DEPC-treated water) and loaded into the gel. After applying 70 V/cm for 25 min, the gel was imaged with ImageQuant LAS 4000 (GE). Analysis of siRNA band intensity was conducted with ImageJ software for quantification. siRNA loading ratio was calculated by comparing the maximum amount of siRNA released from nanoparticles to the nanoparticle mass. Conversion efficiency of siRNA conjugation was calculated by comparing the maximum amount of siRNA released from nanoparticles to the amount of siRNA used to conjugate nanoparticles.

### 3.5. Cells Culture and *in vitro* Assays

Luciferase-expressing HeLa cell line (HeLa/luc) was from Xenogen. HeLa/luc cells were maintained in DMEM high glucose supplemented with 10% FBS, 2 mM L-glutamine, 100 units/mL penicillin and 100 $\mu$g/mL streptomycin, 1 mM sodium pyruvate, and nonessential amino acids. All media and supplements were from GIBCO except for FBS which was from Mediatech, Inc.

HeLa/luc cells were plated in 96-well plates at 5000/well and incubated overnight at 37 °C. Cells were dosed with fluorescently tagged particles in OPTI-MEM (Invitrogen) at 37 °C for 4 h for cell uptake studies. Fluorescently tagged particles were prepared by incorporation of fluorescein *O*-acrylate in the particle composition and copolymerization of these monomers into particle matrix. After incubation, cells were trypsinized and treated with 0.1% trypan blue to quench the fluorescein fluorescence from particles associated with the cell surface. Cells were then washed and fixed in 1% paraformaldehyde/DPBS and analyzed by CyAn ADP flow cytometer (Dako). The cell uptake was represented as the percentage of cells that were positive in fluorescein fluorescence.

For *in vitro* cytotoxicity and luciferase expression assays, cells were dosed with particles or lipofectamine 2000 (Invitrogen)/siRNA (2:1, wt/wt) in OPTI-MEM at 37 °C for 4 h, then particles were removed, and complete grow medium was added for another 48 h incubation at 37 °C. Cell viability was evaluated with Promega CellTiter 96 AQueous One Solution Cell Proliferation Assay, and luciferase expression level was evaluated with Promega Bright-Glo Luciferase Assay according to manufacturer's instructions. Light absorption or bio-luminescence was measured by a SpectraMax M5 plate reader (Molecular Devices). The viability or luciferase expression of the cells exposed to PRINT particles was expressed as a percentage of that of cells grown in the absence of particles. Half-maximal effective concentration ($EC_{50}$) of siRNA required to elicit gene knockdown was determined by applying the dose-dependent luciferase expression data to a log(inhibitor) vs response variable slope nonlinear function in GraphPad Prism software.

### 3.6. Hemolysis Assay

Blood from C57BL/6 mice were washed twice with HBSS buffer. $1.5 \times 10^8$ red blood cells were placed in each well of round-bottom 96-well plate and treated with particle formulations of various concentrations for 30 min at 37 °C. Cells were then centrifuged at 1500 rpm for 10 min, and supernatants were transferred into another plate and absorbance was measured at 540 nm. 0.5% Triton X-100 and 5 mg/mL PEG8000 were used as positive and negative controls, respectively.

### 3.7. Biodistribution of NP in Mice

C57BL/6 mice were intravenously injected with 0.5 mg particles labeled with DyLight 680. Twenty-four h post injections, mice were euthanized, and the major organs (liver, spleen, lung, kidney, and heart) were harvested. The resected organs were imaged by IVIS Lumina fluorescence imaging system (PerkinElmer) with excitation at 675 nm and emission measured at 720 nm. The percentage of NP fluorescence in each organ against the total fluorescence recovered from all the major organs was calculated and presented.

### 3.8. *in vivo* FVII Silencing in Mice

All procedures used in animal studies were approved by the Institutional Animal Care and Use. C57BL/6 mice were from Jackson Laboratories and used at 6–10 weeks old. Particle formulations were administered intravenously via tail vein injection, at 4 or 6 mg siRNA/kg. 48 h post treatment, liver tissues were harvested for analyses.

For qRT-PCR assay of mRNA level, liver tissues were harvested from euthanized mice and preserved in RNALater. qRT-PCR was done as previously published.[41] Primers used were: (Mus Factor VII) forward: ACA AGT CTT ACG TCT GCT TCT; reverse: CAC AGA TCA GCT GCT CAT TCT; probe: FTC TCA CAG TTC CGA CCC TCA AAG TCQ; (Mus $\beta$-Actin) forward: CTG CCT GAC GGC CAG GTC; reverse: CAA GAA GGA AGG CTG GAA AAG A; probe: FCA CTA TTG GCA ACG AGC GGT TCC GQ; F: 5′-fluorescein (FAM); Q: quencher (TAMRA).

FVII protein level in mouse plasma was assayed with BIOPHEN VII assay kit (Aniara Corporation) according to manufacturer's instructions. A standard curve was constructed using samples from PBS-injected mice and relative Factor VII expression was determined by comparing treated groups to untreated PBS control.

For immunohistochemistry analysis, particles were labeled with DyLight 680 dye. Particle formulations were administered intravenously via tail vein injection, at 4 mg siRNA/kg. Twenty-four h post treatment, liver tissues were harvested and snap frozen in O.C.T medium and cryosected into 5 $\mu$m sections. Sections were fixed in ice cold acetone for 5 min, briefly air-dried, and rehydrated in 1× PBS for 15 min. The tissue sections were then blocked with 1% bovine serum albumin in PBS for 20 min, and sequentially stained with antimouse MARCO (Invitrogen) and goat antirat IgG-Alexa Fluor 488 in 1% BSA/PBS. Tissue sections were also stained with phalloidin-Alexa Fluor 555 (Invitrogen) and DAPI (Sigma). Images were collected with Zeiss710 confocal laser scanning microscope (Carl Zeiss).

### 3.9. Statistical Analysis

Liver FVII mRNA and plasma FVII protein measurements were analyzed by One-Way ANOVA followed by Bonferroni's Multiple Comparison test.

# 4. RESULTS AND DISCUSSION

## 4.1. Nanoparticle Preparation and Characterization

We chose to make a rod-shaped particle with high aspect ratio: 80 × 80 × 320 nm (*L* × *W* × *H*, 80 × 320 nm hereafter) for enhanced cell uptake[42] and improved *in vivo* PK previously[40,43] compared to 200 × 200 cylindrical particles we previously used for siRNA delivery.[37] Compared to the direct siRNA incorporation method previously reported,[37] the current formulation strategy made particles and loaded siRNA in two separate steps. We first prepared 80 × 320 nm hydrogel nanoparticles using the PRINT based continuous particle fabrication instrument with a high efficiency.[40] A representative "blank" nanoparticle composition (Table S1) includes: (1) AEM (2-aminoethyl methacrylate) as a reaction handle for siRNA conjugation; (2) cationic tertiary amine DMAPMA (*N*-[3-(dimethylamino)propyl]methacrylamide) to improve transfection efficiency; (3) $mPEG_{5k}$-acrylate as a nanoparticle stabilizer. This composition also includes cross-linker ($PEG_{700}$ diacrylate), photo initiator (TPO), and hydrophile (tetra-ethylene glycol monoacrylate). This composition dissolved in volatile methanol is fully compatible with mold based continuous fabrication process without using aqueous content for siRNA dissolution. 300 mg of nanoparticles with highly uniform size, shape, and composition were prepared within 30 min. As illustrated in Scheme 1, the resulting "blank" nanoparticles were treated with SPDP (succinimidyl 3-(2-pyridyldithio)propionate),[44] which reacted with primary amine groups on nanoparticles. Subsequently, by incubating these nanoparticles in thiol modified siRNA (siRNA modification method described in the Supporting Information),[45] siRNA was conjugated to nanoparticles via a disulfide linker to enable reduction-sensitive release of cargo. To further enhance transfection efficiency, nanoparticles were treated with polyammonium polymers (poly-L-lysine) along with an activation agent of EDC (1-Ethyl-3-(3-(dimethylamino)-propyl)carbodiimide) and sulfo-NHS (*N*-hydroxysulfosuccinimide sodium salt). The SEM micrograph (Figure 1a and S1) indicated that the size, shape, and integrity of these rod-shape nanoparticles were well-retained after siRNA loading and surface modification. Dynamic light scattering measurement in water using a mathematical model of spherical particles indicated that the 80 × 320 nm rod-shape nanoparticles had an overall hydrodynamic size of 368.2 ± 4.2 nm with a narrow size distribution (PDI = 0.06).

## 4.2. Reductively Responsive Release of siRNA

Electrostatic complexation of siRNA with cationic nanoparticles may have the issue of premature release during circulation in blood. In order to avoid this issue, siRNA was conjugated to hydrogel nanoparticles via a "pro-drug" strategy. The disulfide linker in these "pro-siRNA" hydrogel nanoparticles is stable in the physiological environment, but cleavable in the intracellular reducing environment. As shown in Figure 1b, these reductively responsive hydrogel nanoparticles are expected to maintain encapsulation of siRNA while circulating in blood and release the cargo after entering cells. The release profile of siRNA loaded nanoparticles is shown in Figure 1c. While no siRNA was released in PBS, siRNA was quickly released when incubated in 5 mM glutathione,[46] which mimics the intracellular reducing condition.[37]

### 4.3. Protection of siRNA from Degradation

Another important requirement for siRNA carriers is the capability to protect cargo from degradation by RNase. To determine if hydrogel nanoparticles provided conjugated siRNA protection from nuclease degradation, a stability assay was carried out. As shown in Figure 1d, siRNA conjugated to hydrogel nanoparticles was stable after incubation in 30% FBS for 24 h. By comparison, naked siRNA was completely degraded by 30% FBS in the same period of incubation.

### 4.4. siRNA Delivery Evaluation *in vitro*

Before these siRNA conjugated nanoparticles were used for systemic delivery *in vivo*, nanoparticle composition was adjusted to evaluate gene silencing efficiency *in vitro*. PEG-based PRINT hydrogel particles without targeting ligand generally enter nonphagocytic cells via endocytosis.[42] Positive charges of cationic nanoparticles enhance nonspecific interactions with cells, improve endocytosis, and assist endosomal escape likely via so-called “proton sponge” effect.[37,47,48] We were able to tune the positive charge density of these nanoparticles by varying their composition and surface modification of PLLs. Luciferase gene silencing was evaluated by treating HeLa/luc cells with luciferase–siRNA conjugated nanoparticles of different surface modifications, chemical compositions, and siRNA loading ratios.

First, three PLLs of different molecular weights (1–5k, 15–30k, and 30–70k) were used to modify nanoparticle surface properties, when the content of the tertiary amine macromer DMAPMA was fixed at 40 wt % and siRNA was constantly charged at 40 wt %. Luciferase expressing HeLa/luc cells were treated with luciferase-siRNA conjugated nanoparticles in a media with reduced serum (OPTI-MEM) for 4 h. Nanoparticles were subsequently removed, and cells were incubated at 37 °C for another 48 h. Dose-dependent knock-down of luciferase expression was observed with a maximum gene silencing of 90%, when nanoparticles were surface modified with PLL 15–30k (Figure 2a). Nanoparticles modified with PLL 15–30k showed no cytotoxicity (Figure 2b). By 30k. Four different ratios of siRNA (weight percentage to “blank” nanoparticles), 100, 40, 20, and 10 wt %, were charged and conjugated to “blank” nanoparticles. The siRNA loading ratios of the resulting nanoparticles were 18.2, 10.0, 5.8, and 2.6 wt %, respectively (Table 1). The loading efficiencies of siRNA comparison, nanoparticles modified with PLL 1–5k showed low transfection efficiency, and nanoparticles modified with the large molecular weight PLL (30–70k) led to high cytotoxicity.

Next, the content of the tertiary amine macromer DMAPMA was varied with the siRNA charging ratio fixed at 40 wt % and surface modification with PLL 15–30k. The dimethyl amine group in DMAPMA may assist cellular uptake and increases pH buffering capacity to enhance endosomal escape due to the “proton sponge” effect. Luciferase transfected HeLa cells were dosed with hydrogel nanoparticles fabricated with different DMAPMA contents of 10, 20, and 40 wt % (weight percent to macromers in preparticle solution). As illustrated in Figure 2c (cell uptake and viability assays are shown in Figure S4 and S5), nanoparticles with the highest DMAPMA content of 40 wt % had the highest transfection efficiency, while those with 10 and 20 wt % DMAPMA were less efficient in delivering luciferase-siRNA

into HeLa/luc cells. Therefore, we chose 40 wt % DMAPMA as the best nanoparticle composition to enhance transfection.

Furthermore, nanoparticles were conjugated with different ratios of siRNA to evaluate the influence of siRNA loading ratio on transfection efficiency. “Blank” nanoparticles were fabricated with 40 wt % DMAPMA and surface modified with PLL 15–30k. Four different ratios of siRNA (weight percentage to “blank” nanoparticles), 100, 40, 20, and 10 wt %, were charged and conjugated to “blank” nanoparticles. The siRNA loading ratios of the resulting nanoparticles were 18.2, 10.0, 5.8, and 2.6 wt %, respectively (Table 1). The loading efficiencies of siRNA were between 18% and 29%. Silencing of luciferase expression with hydrogel nanoparticles of different siRNA loading ratios was evaluated (Figure 2d). $EC_{50}$ was calculated to be 509, 150, 116, and 80 nM, respectively. Nanoparticles with the lowest siRNA loading ratio had the lowest $EC_{50}$ and were the most efficient at gene silencing based on the amount of siRNA dosed. It is possible that, with a large quantity of siRNA conjugated (up to 18 wt %), the relatively lower content of cationic polymers would lower the transfection efficiency, including less efficient cellular uptake and reduced endosomal escape capability. The highest transfection efficiency achieved by our hydrogel nanoparticles ($EC_{50}$ = 80 nM) is comparable to that achieved by lipofectamine 2000 ($EC_{50}$ = 28 nM, Figure S6), a commercially available transfection agent, which is widely used for *in vitro* transfection. We chose nanoparticles loaded with 10.0 wt % siRNA, which combined a high loading ratio and efficient gene silencing, for further *in vivo* animal studies.

### 4.5. siRNA Delivery *in vivo*

The above studies indicate that hydrogel nanoparticles with surface modification of PLL 15–30k, chemical composition of 40 wt % DMAPMA, and siRNA loading ratio of 10 wt % achieved efficient transfection *in vitro* in a media with reduced serum (OPTI-MEM). Nanoparticles of this composition were positively charged ($\zeta$-potential = +31.8 mV). Positive nanoparticles may suffer from reduced transfection efficiency in serum-containing medium as a result of serum protein coating. The coating with negatively charged serum protein would change the nanoparticle surface property and significantly lower the capability of cellular uptake and endosomal escape. Notably, the luciferase expression assay of our luciferase–siRNA conjugated nanoparticles showed no reduction in transfection efficiency in 10% FBS compared to those in medium with reduced serum (Figure S7). This result demonstrated that nanoparticles were stabilized, most likely by $mPEG_{5k}$ acrylate used to fabricate “blank” nanoparticles and/or NHS-$PEG_{3.4k}$-COOH used to modify the nanoparticle surface.

The above formulation was used for systemic delivery *in vivo*. Cationic nanoparticles could be subject to quick clearance during circulation in blood due to opsonization.[49] Our previous study demonstrated that PEGylation of hydrogel NP significantly improved circulation of NP.[40] Therefore, mPEG modified poly(acrylic acid) ($mPEG_{5k}$-PAA) was used to coat siRNA loaded cationic nanoparticles to further stabilize them for *in vivo* applications. The resulting nanoparticles had a slightly negative $\zeta$-potential of −5.8 mV and a size of 331.5 ± 4.4 nm (PDI = 0.06) in 0.1× PBS (pH = 7.4). Distribution study of the cationic NP and $mPEG_{5k}$-

PAA coated NP in mice showed that both accumulated most efficiently in liver (>40%), followed by accumulation in spleen and kidney at similar levels (Figure S8). About 20% of cationic NP was also found in lung, likely due to opsonization of positively charged NP in blood and formation of larger aggregates, which is often filtered by lung. On the other hand, only 5% of $mPEG_{5k}$-PAA coating was in lung, and there was about 10% more of this NP in liver instead. Further examination of liver sections (Figure S9) indicated that $mPEG_{5k}$-PAA coating helps to stabilize NP *in vivo* and get internalized by hepatocytes and other liver cells, while cationic NP tended to aggregate and was less taken up by cells.

The toxicity of these $mPEG_{5k}$-PAA coated nanoparticles to red blood cells was studied with a hemolysis assay (Figure 3a). Red blood cells (RBCs) were treated with hydrogel nanoparticles at 0.111, 0.333, and 1 mg/mL and incubated at 37 °C for 0.5 h. Minimal RBC lysis was observed with up to 1 mg/mL of either FVII-siRNA or luciferase-siRNA conjugated nanoparticles. This result indicates these nanoparticles have minimal toxicity to red blood cells when administered for systemic delivery.

Studies have been reported on using siRNA to treat liver-related diseases.[49,50] Since biodistribution study as well as liver examination indicated efficient accumulation of our hydrogel particles in liver parenchymal cells, we chose to show the gene silencing potential of this system in liver in the initial investigation. Coagulation factor VII (FVII) that is produced by liver hepatocytes has been reported in multiple siRNA delivery systems.[8,51–53] In addition, measurements of FVII at mRNA and blood protein levels have been well studied. Therefore, mouse hepatic FVII was chosen as the gene target to test the efficacy of siRNA delivery and gene silencing. Mice were dosed with FVII-siRNA loaded nanoparticles via intravenous administration at 6 mg/kg or 4 mg/kg (weight ratio of siRNA to mice). Nanoparticles loaded with luciferase-siRNA were administered at the same dose as the control. Liver tissues and blood were collected 48 h post treatments for mRNA and FVII protein analyses, respectively. Figure 3b showed that 6 mg/kg FVII-siRNA resulted in ~75% reduction of the FVII mRNA level, while the lower dose of 4 mg/kg FVII-siRNA gave a moderate reduction of approximately 40%. The reduction of the FVII protein level in plasma followed the same trend, with 6 mg/kg FVII-siRNA administration leading to a 40% decrease in FVII protein level in blood (Figure S10). Since protein is more stringently regulated, the decrease in protein level is smaller compared to that of mRNA level. Optimization of treatment regime may be needed for desired knockdown levels.

A closer examination of liver tissues from mice treated with hydrogel nanoparticles (labeled with DyLight 680 and loaded with FVII-siRNA) via intravenous administration was done by confocal microscopy. Figure 3c showed a representative image of liver sections from mice treated with nanoparticles (separate channels shown in Figure S11). It could be seen that large quantities of particles (green) were accumulated in almost all cells, including Kupffer cells (magenta) and other cells (red) which should be mostly hepatocytes, the mesenchymal cells of liver (70–85% of total liver cells). In addition, images taken along *z*-axis showed that particles were distributed at different depth of tissues (Figure S12), further demonstrating that the particles were able to penetrate liver tissues and reach intracellular environment. These results together demonstrated the capability of the nanoparticles to deliver cargo to liver hepatocytes and silence gene expression.

## 5. CONCLUSION

siRNA conjugated polymeric nanoparticles with a uniform shape, size, and composition have been developed and used for systemic delivery *in vivo*. Building on our previous work, the new "post-fabrication" siRNA loading method allows us to use PRINT based continuous particle fabrication to prepare large quantity of nanoparticles with a high efficiency. The cargo was conjugated to nanoparticles with a loading ratio of up to 18 wt % and a loading efficiency of up to 29%. The composition, surface modification, and siRNA conjugation ratio of nanoparticles are highly tunable to achieve efficient luciferase gene silencing *in vitro* with minimum cytotoxicity. Furthermore, FVII-siRNA loaded nanoparticles are capable of efficient knock-down of FVII expression via systemic delivery *in vivo*. We are currently further optimizing this hydrogel formulation for other targets, including tumors, and also developing particles constituted with biodegradable materials.

## Supplementary Material

Refer to Web version on PubMed Central for supplementary material.

## ACKNOWLEDGMENTS

We thank Jillian Perry, Charlie Bowerman, and Kevin Reuter for assisting nanoparticle fabrication, Raju Krishna Kumar and Julie Mabile for siRNA synthesis, Gabriel Gamber, Cameron Lee, David Morrissey, Chandra Vargeese, Keith Bowman, and Stphany Standley for discussions. This work is financially supported by National Institutes of Health.

## REFERENCES

(1). Fire A, Xu S, Montgomery MK, Kostas SA, Driver SE, Mello CC. Potent and Specific Genetic Interference by Double-Stranded RNA in Caenorhabditis Elegans. Nature. 1998; 391:806–811. [PubMed: 9486653]

(2). Elbashir SM, Lendeckel W, Tuschl T. RNA Interference Is Mediated by 21- and 22-Nucleotide RNAs. Genes Dev. 2001; 15:188–200. [PubMed: 11157775]

(3). Davis ME, Zuckerman JE, Choi CHJ, Seligson D, Tolcher A, Alabi CA, Yen Y, Heidel JD, Ribas A. Evidence of RNAi in Humans from Systemically Administered siRNA via Targeted Nanoparticles. Nature. 2010; 464:1067–1070. [PubMed: 20305636]

(4). Whitehead KA, Langer R, Anderson DG. Knocking down Barriers: Advances in siRNA Delivery. Nat. Rev. Drug Discovery. 2009; 8:129–138. [PubMed: 19180106]

(5). Buyens K, De Smedt SC, Braeckmans K, Demeester J, Peeters L, van Grunsven LA, de Mollerat du Jeu X, Sawant R, Torchilin V, Farkasova K, Ogris M, Sanders NN. Liposome Based Systems for Systemic siRNA Delivery: Stability in Blood Sets the Requirements for Optimal Carrier Design. J. Controlled Release. 2012; 158:362–370.

(6). Landen CN, Chavez-Reyes A, Bucana C, Schmandt R, Deavers MT, Lopez-Berestein G, Sood AK. Therapeutic EphA2 Gene Targeting *in vivo* Using Neutral Liposomal Small Interfering RNA Delivery. Cancer Res. 2005; 65:6910–6918. [PubMed: 16061675]

(7). Alabi, C. a; Love, KT.; Sahay, G.; Yin, H.; Luly, KM.; Langer, R.; Anderson, DG. Multiparametric Approach for the Evaluation of Lipid Nanoparticles for siRNA Delivery. Proc. Natl. Acad. Sci. U. S. A. 2013; 110:12881–12886. [PubMed: 23882076]

(8). Akinc A, Zumbuehl A, Goldberg M, Leshchiner ES, Busini V, Hossain N, Bacallado SA, Nguyen DN, Fuller J, Alvarez R, Borodovsky A, Borland T, Constien R, de Fougerolles A, Dorkin JR, Narayanannair Jayaprakash K, Jayaraman M, John M, Koteliansky V, Manoharan M, Nechev L, Qin J, Racie T, Raitcheva D, Rajeev KG, Sah DWY, Soutschek J, Toudjarska I, Vornlocher H-P,

Zimmermann TS, Langer R, Anderson DG. A Combinatorial Library of Lipid-like Materials for Delivery of RNAi Therapeutics. Nat. Biotechnol. 2008; 26:561–569. [PubMed: 18438401]

(9). Komisarski M, Osornio YM, Siegel JS, Landau EM. Tailored Host-Guest Lipidic Cubic Phases: A Protocell Model Exhibiting Nucleic Acid Recognition. >Chem. - Eur. J. 2013; 19:1262–1267. [PubMed: 23239006]

(10). Angelov B, Angelova A, Filippov SK, Narayanan T, Drechsler M, Štěpánek P, Couvreur P, Lesieur S. DNA/fusogenic Lipid Nanocarrier Assembly: Millisecond Structural Dynamics. J. Phys. Chem. Lett. 2013; 4:1959–1964. [PubMed: 26283134]

(11). Angelov B, Angelova A, Filippov SK, Karlsson G, Terrill N, Lesieur S, Štěpánek P. Topology and Internal Structure of PEGylated Lipid Nanocarriers for Neuronal Transfection: Synchrotron Radiation SAXS and Cryo-TEM Studies. Soft Matter. 2011; 7:9714–9720.

(12). Angelova A, Angelov B, Drechsler M, Lesieur S. Neurotrophin Delivery Using Nanotechnology. Drug Discovery Today. 2013; 18:1263–1271. [PubMed: 23891881]

(13). Oliveira ACN, Martens TF, Raemdonck K, Adati RD, Feitosa E, Botelho C, Gomes AC, Braeckmans K, Real Oliveira MECD. Dioctadecyldimethylammonium:monoolein Nanocarriers for Efficient *in vitro* Gene Silencing. ACS Appl. Mater. Interfaces. 2014; 6:6977–6989. [PubMed: 24712543]

(14). Borgheti-Cardoso LN, Depieri LV, Diniz H, Calzzani RAJ, De Abreu Fantini MC, Iyomasa MM, Moura De Carvalho Vicentini FT, Bentley MVLB. Self-Assembling Gelling Formulation Based on a Crystalline-Phase Liquid as a Non-Viral Vector for siRNA Delivery. Eur. J. Pharm. Sci. 2014; 58:72–82. [PubMed: 24726985]

(15). Angelova A, Angelov B, Mutafchieva R, Lesieur S. Biocompatible Mesoporous and Soft Nanoarchitectures. J. Inorg. Organomet. Polym. Mater. 2015; 25:214–232.

(16). Angelov B, Angelova A, Drechsler M, Garamus VM, Mutafchieva R, Lesieur S. Identification of Large Channels in Cationic PEGylated Cubosome Nanoparticles by Synchrotron Radiation SAXS and Cryo-TEM Imaging. Soft Matter. 2015; 11:3686–3692. [PubMed: 25820228]

(17). Gindy ME, Difelice K, Kumar V, Prud'homme RK, Celano R, Haas RM, Smith S, Boardman D. Mechanism of Macromolecular Structure Evolution in Self- Assembled Lipid Nanoparticles for siRNA Delivery. Langmuir. 2014; 30:4613–4622. [PubMed: 24684657]

(18). Shrestha R, Elsabahy M, Florez-Malaver S, Samarajeewa S, Wooley KL. Endosomal Escape and siRNA Delivery with Cationic Shell Crosslinked Knedel-like Nanoparticles with Tunable Buffering Capacities. Biomaterials. 2012; 33:8557–8568. [PubMed: 22901966]

(19). Patil ML, Zhang M, Taratula O, Garbuzenko OB, He H, Minko T. Internally Cationic Polyamidoamine PAMAM-OH Dendrimers for siRNA Delivery: Effect of the Degree of Quaternization and Cancer Targeting. Biomacromolecules. 2009; 10:258–266. [PubMed: 19159248]

(20). Hasan W, Chu K, Gullapalli A, Dunn SS, Enlow EM, Luft JC, Tian S, Napier ME, Pohlhaus PD, Rolland JP, DeSimone JM. Delivery of Multiple siRNAs Using Lipid-Coated PLGA Nanoparticles for Treatment of Prostate Cancer. Nano Lett. 2012; 12:287–292. [PubMed: 22165988]

(21). Ornelas-Megiatto C, Wich PR, Fréchet JMJ. Polyphosphonium Polymers for siRNA Delivery: An Efficient and Nontoxic Alternative to Polyammonium Carriers. J. Am. Chem. Soc. 2012; 134:1902–1905. [PubMed: 22239619]

(22). Gu W, Jia Z, Truong NP, Prasadam I, Xiao Y, Monteiro MJ. Polymer Nanocarrier System for Endosome Escape and Timed Release of siRNA with Complete Gene Silencing and Cell Death in Cancer Cells. Biomacromolecules. 2013; 14:3386–3389. [PubMed: 23992391]

(23). Truong NP, Gu W, Prasadam I, Jia Z, Crawford R, Xiao Y, Monteiro MJ. An Influenza Virus-Inspired Polymer System for the Timed Release of siRNA. Nat. Commun. 2013; 4:1902. [PubMed: 23695696]

(24). Van Asbeck AH, Beyerle A, McNeill H, Bovee-Geurts PHM, Lindberg S, Verdurmen WPR, Hallbrink M, Langel U, Heidenreich O, Brock R. Molecular Parameters of siRNA–Cell Penetrating Peptide Nanocomplexes for Efficient Cellular Delivery. ACS Nano. 2013; 7:3797–3807. [PubMed: 23600610]

(25). Ren Y, Hauert S, Lo JH, Bhatia SN. Identification and Characterization of Receptor-Specific Peptides for siRNA Delivery. ACS Nano. 2012; 6:8620–8631. [PubMed: 22909216]

(26). Li J, Chen YC, Tseng YC, Mozumdar S, Huang L. Biodegradable Calcium Phosphate Nanoparticle with Lipid Coating for Systemic siRNA Delivery. J. Controlled Release. 2010; 142:416–421.

(27). Zhang M, Ishii A, Nishiyama N, Matsumoto S, Ishii T, Yamasaki Y, Kataoka K. PEGylated Calcium Phosphate Nanocomposites as Smart Environment-Sensitive Carriers for siRNA Delivery. Adv. Mater. 2009; 21:3520–3525.

(28). Giljohann DA, Seferos DS, Prigodich AE, Patel PC, Mirkin CA. Gene Regulation with Polyvalent siRNA-Nanoparticle Conjugates. J. Am. Chem. Soc. 2009; 131:2072–2073. [PubMed: 19170493]

(29). Kam NWS, Liu Z, Dai H. Functionalization of Carbon Nanotubes via Cleavable Disulfide Bonds for Efficient Intracellular Delivery of siRNA and Potent Gene Silencing. J. Am. Chem. Soc. 2005; 127:12492–12493. [PubMed: 16144388]

(30). Nelson CE, Kintzing JR, Hanna A, Shannon JM, Gupta MK, Duvall CL. Balancing Cationic and Hydrophobic Content of PEGylated siRNA Polyplexes Enhances Endosome Escape, Stability, Blood Circulation Time, and Bioactivity *in vivo*. ACS Nano. 2013; 7:8870–8880. [PubMed: 24041122]

(31). Li J, Yang Y, Huang L. Calcium Phosphate Nanoparticles with an Asymmetric Lipid Bilayer Coating for siRNA Delivery to the Tumor. J. Controlled Release. 2012; 158:108–114.

(32). Rolland JP, Maynor BW, Euliss LE, Exner AE, Denison GM, DeSimone JM. Direct Fabrication and Harvesting of Monodisperse, Shape-Specific Nanobiomaterials. J. Am. Chem. Soc. 2005; 127:10096–10100. [PubMed: 16011375]

(33). Petros RA, Ropp PA, DeSimone JM. Reductively Labile PRINT Particles for the Delivery of Doxorubicin to HeLa Cells. J. Am. Chem. Soc. 2008; 130:5008–5009. [PubMed: 18355010]

(34). Merkel TJ, Jones SW, Herlihy KP, Kersey FR, Shields AR, Napier M, Luft JC, Wu H, Zamboni WC, Wang AZ, Bear JE, DeSimone JM. Using Mechanobiological Mimicry of Red Blood Cells to Extend Circulation Times of Hydrogel Microparticles. Proc. Natl. Acad. Sci. U. S. A. 2011; 108:586–591. [PubMed: 21220299]

(35). Wang J, Tian S, Petros RA, Napier ME, Desimone JM. The Complex Role of Multivalency in Nanoparticles Targeting the Transferrin Receptor for Cancer Therapies. J. Am. Chem. Soc. 2010; 132:11306–11313. [PubMed: 20698697]

(36). Xu J, Wang J, Luft JC, Tian S, Owens G Jr. Pandya AA, Berglund P, Pohlhaus P, Maynor BW, Smith J, Hubby B, Napier ME, DeSimone JM. Rendering Protein-Based Particles Transiently Insoluble for Therapeutic Applications. J. Am. Chem. Soc. 2012; 134:8774–8777. [PubMed: 22568387]

(37). Dunn SS, Tian S, Blake S, Wang J, Galloway AL, Murphy A, Pohlhaus PD, Rolland JP, Napier ME, DeSimone JM. Reductively Responsive siRNA-Conjugated Hydrogel Nanoparticles for Gene Silencing. J. Am. Chem. Soc. 2012; 134:7423–7430. [PubMed: 22475061]

(38). Canelas DA, Herlihy KP, DeSimone JM. Top-down Particle Fabrication: Control of Size and Shape for Diagnostic Imaging and Drug Delivery. Wiley Interdiscip. Rev. Nanomedicine Nanobiotechnology. 2009; 1:391–404.

(39). Guzmán J, Iglesias MT, Riande E, Compañ V, Andrio A. Synthesis and Polymerization of Acrylic Monomers with Hydrophilic Long Side Groups. Oxygen Transport through Water Swollen Membranes Prepared from These Polymers. Polymer. 1997; 38:5227–5232.

(40). Perry JL, Reuter KG, Kai MP, Herlihy KP, Jones SW, Luft JC, Napier M, Bear JE, DeSimone JM. PEGylated PRINT Nanoparticles: The Impact of PEG Density on Protein Binding, Macrophage Association, Biodistribution, and Pharmacokinetics. Nano Lett. 2012; 12:5304–5310. [PubMed: 22920324]

(41). Kim H-S, Lee G, John SWM, Maeda N, Smithies O. Molecular Phenotyping for Analyzing Subtle Genetic Effects in Mice: Application to an Angiotensinogen Gene Titration. Proc. Natl. Acad. Sci. U. S. A. 2002; 99:4602–4607. [PubMed: 11904385]

(42). Gratton SEA, Ropp PA, Pohlhaus PD, Luft JC, Madden VJ, Napier ME, DeSimone JM. The Effect of Particle Design on Cellular Internalization Pathways. Proc. Natl. Acad. Sci. U. S. A. 2008; 105:11613–11618. [PubMed: 18697944]

(43). Chu KS, Hasan W, Rawal S, Walsh MD, Enlow EM, Luft JC, Bridges AS, Kuijer JL, Napier ME, Zamboni WC, DeSimone JM. Plasma, Tumor and Tissue Pharmacokinetics of Docetaxel Delivered via Nanoparticles of Different Sizes and Shapes in Mice Bearing SKOV-3 Human Ovarian Carcinoma Xenograft. Nanomedicine. 2013; 9:686–693. [PubMed: 23219874]

(44). Kim SH, Jeong JH, Lee SH, Kim SW, Park TG. PEG Conjugated VEGF siRNA for Anti-Angiogenic Gene Therapy. J. Controlled Release. 2006; 116:123–129.

(45). Shin IS, Jang B, Danthi SN, Xie J, Yu S, Le N, Maeng J, Hwang IS, Li KCP, Carrasquillo JA, Paik CH. Use of Antibody as Carrier of Oligomers of Peptidomimetic R v Target Tumor-Induced Neovasculature Antagonist to. Bioconjugate Chem. 2007; 18:821–828.

(46). Hwang C, Sinskey AJ, Lodish HF. Oxidized Redox State of Glutathione in the Endoplasmic Reticulum. Science. 1992; 257:1496–1502. [PubMed: 1523409]

(47). Ma D. Enhancing Endosomal Escape for Nanoparticle Mediated siRNA Delivery. Nanoscale. 2014; 6:6415–6425. [PubMed: 24837409]

(48). Behr J. The Proton Sponge: A Trick to Enter Cells the Viruses Did Not Exploit. Chim. Int. J. Chem. 1997; 2:34–36.

(49). Nel AE, Mädler L, Velegol D, Xia T, Hoek EMV, Somasundaran P, Klaessig F, Castranova V, Thompson M. Understanding Biophysicochemical Interactions at the Nano-Bio Interface. Nat. Mater. 2009; 8:543–557. [PubMed: 19525947]

(50). Rozema DB, Lewis DL, Wakefield DH, Wong SC, Klein JJ, Roesch PL, Bertin SL, Reppen TW, Chu Q, Blokhin AV, Hagstrom JE, Wolff JA. Dynamic PolyConjugates for Targeted *in vivo* Delivery of siRNA to Hepatocytes. Proc. Natl. Acad. Sci. U. S. A. 2007; 104:12982–12987. [PubMed: 17652171]

(51). Akinc A, Querbes W, De S, Qin J, Frank-Kamenetsky M, Jayaprakash KN, Jayaraman M, Rajeev KG, Cantley WL, Dorkin JR, Butler JS, Qin L, Racie T, Sprague A, Fava E, Zeigerer A, Hope MJ, Zerial M, Sah DWY, Fitzgerald K, Tracy MA, Manoharan M, Koteliansky V, de Fougerolles A, Maier MA. Targeted Delivery of RNAi Therapeutics with Endogenous and Exogenous Ligand-Based Mechanisms. Mol. Ther. 2010; 18:1357–1364. [PubMed: 20461061]

(52). Wooddell CI, Rozema DB, Hossbach M, John M, Hamilton HL, Chu Q, Hegge JO, Klein JJ, Wakefield DH, Oropeza CE, Deckert J, Roehl I, Jahn-Hofmann K, Hadwiger P, Vornlocher H-P, McLachlan A, Lewis DL. Hepatocyte-Targeted RNAi Therapeutics for the Treatment of Chronic Hepatitis B Virus Infection. Mol. Ther. 2013; 21:973–985. [PubMed: 23439496]

(53). Jayaraman M, Ansell SM, Mui BL, Tam YK, Chen J, Du X, Butler D, Eltepu L, Matsuda S, Narayanannair JK, Rajeev KG, Hafez IM, Akinc A, Maier MA, Tracy MA, Cullis PR, Madden TD, Manoharan M, Hope MJ. Maximizing the Potency of siRNA Lipid Nanoparticles for Hepatic Gene Silencing *in vivo*. Angew. Chem., Int. Ed. 2012; 51:8529–8533.

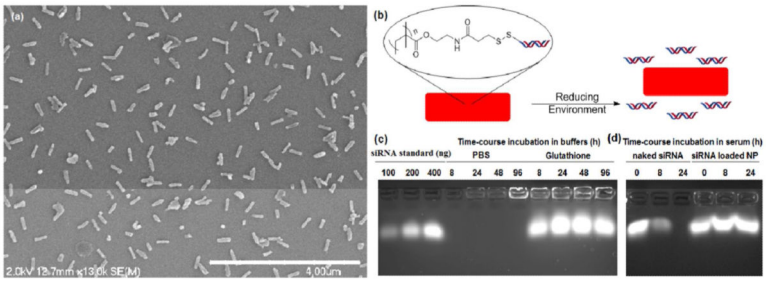


**Figure 1.**

(a) SEM micrograph of 80 × 320 nm hydrogel nanoparticles conjugated with siRNA (scale bar 4 $\mu$m); (b) illustration of reductively responsive hydrogel behavior under physiological and intracellular conditions; (c) time-dependent incubation of pro-siRNA hydrogels (1 mg/mL) in PBS and under reducing conditions (glutathione, 5 mM) at 37 °C; (d) Integrity of siRNA soluble or conjugated to hydrogels after exposure to 30% fetal bovine serum (FBS) in PBS over time; after FBS treatment, siRNA was extracted from nanoparticles using 5 mM glutathione in 10× PBS and analyzed with gel electrophoresis.

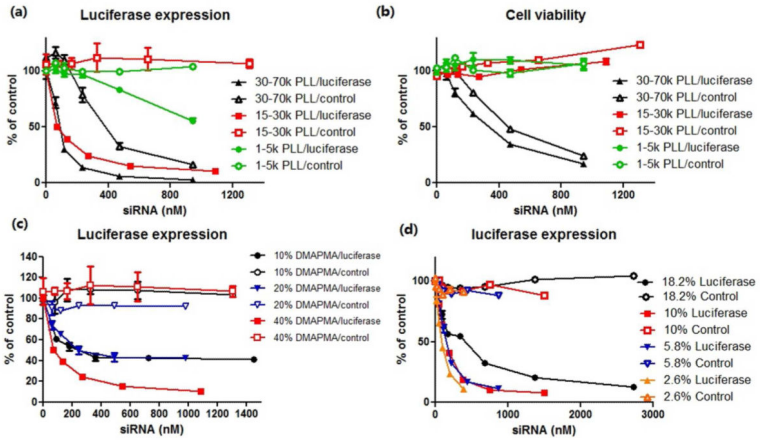


**Figure 2.**

(a) Luciferase expression and (b) viability of Hela/luc cells treated with cationic hydrogel nanoparticles surface modified with PLL of different molecular weights. Luciferase expression in HeLa/luc cells treated with nanoparticles of (c) different tertiary amine DMAPMA contents and (d) different siRNA loading ratios. Cells were dosed with nanoparticles in a media with reduced serum (OPTI-MEM) for 4 h followed by the removal of nanoparticles and 48 h incubation in media. The error bars represent standard deviation from triplicate wells in the same experiment. The amount of siRNA loaded was calculated based on that was released in gel electrophoresis assays. Nonspecific siRNA was used as a control.

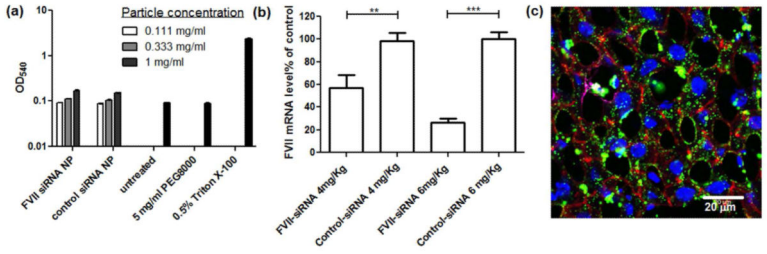


**Figure 3.**

(a) Hemolysis assay with mPEG-PAA coated and FVII-siRNA or control-siRNA conjugated nanoparticles at 0.111, 0.333, and 1 mg/mL; 0.5% Triton X-100 was used as the positive control, and 5 mg/mL $PEG_{8000}$ as the negative control. *in vivo* FVII knock-down (48 h after intravenous administration) with different doses of FVII-siRNA or control-siRNA conjugated nanoparticles: (b) FVII mRNA level in liver with qRT-PCR assay. (c) Confocal micrograph of liver tissue (24 h after intravenous administration of nanoparticles) from mice treated with DyLight 680 labeled nanoparticles (green). Cellular actin cytoskeleton was stained with phalloidin (red), macrophages with MARCO (magenta), and nuclei with DAPI (blue). Scale bar represents 20 $\mu$m. Antiluciferase siRNA conjugated nanoparticles were used as the control. Results are combinations of two independent experiments with $n = 4–5$ for each experiment; data are shown as mean ± SEM $^{*}p < 0.05$; $^{**}p < 0.01$; $^{***}p < 0.001$.

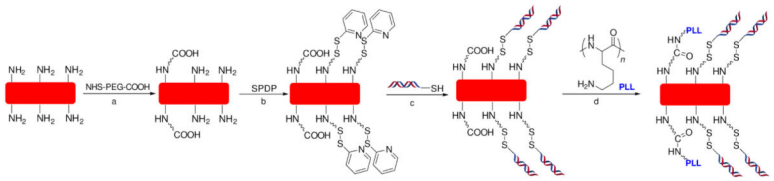


**Scheme 1.**

Schematic Illustration of “Post-Fabrication” siRNA Loading and Surface Modification: (a) NHS-$PEG_{3.4k}$-COOH, DMF, Pyridine; (b) SPDP, PBS/$CH_3CN$; (c) siRNA-SH, PBS; (d) Poly-L-lysine, EDC, Sulfo-NHS, PBS

**Table 1**

siRNA Loading Ratio, Loading Efficiency, and $EC_{50}$ of Nanoparticles Charged with Different Amounts of siRNA

| theoretical siRNA charging ratio | empirical measured siRNA loading ratio | loading efficiency | $EC_{50}$ (nM) |
|---|---|---|---|
| 100 wt % | 18.2 wt % | 18% | 509 |
| 40 wt % | 10.0 wt % | 25% | 150 |
| 20 wt % | 5.8 wt % | 29% | 116 |
| 10 wt % | 2.6 wt % | 26% | 80 |